Acta Crystallographica Section B
**Structural
Science**
ISSN 0108-7681

CH_3CN: X-ray structural investigation of a unique single crystal. $\beta \rightarrow \alpha$ phase transition and crystal structure

Renée Enjalbert* and Jean Galy

Centre d'Elaboration de Matériaux et d'Etudes Structurales, 29 Rue Jeanne Marvig, BP 4347, 31055 Toulouse CEDEX 04, France

Correspondence e-mail: galy@cemes.fr

Received 7 June 2002
Accepted 25 September 2002

The phase transition from the low- (β) to the high-temperature (α) form of acetonitrile, CH_3CN, has been directly observed and studied on a unique single crystal. Both the β and α structures have been determined at temperatures close to the transition temperature (206 K and 201 K), taking advantage of the hysteresis. A single crystal of the β form was obtained for the first time.

1. Introduction

Acetonitrile, CH_3CN, is an important basic solvent in organic and coordination chemistry. As a polar liquid it exhibits a rather high boiling point (354.6 K), which is related to the fact that the large dipole moment of the molecule induces dipole–dipole interactions between pairs of molecules. The melting point of CH_3CN is 227 K. In the solid state, CH_3CN exists in two forms, α and β, with a phase transition occurring at 216.9 K as determined by Putnam *et al.* (1965).

Both the α and β structures have been studied. Barrow (1981) studied the α form at 215 K, using equi-inclination multiple-film packing methods (Cu $K\alpha$), the acetonitrile being sealed in a Lindeman capillary. Brackmeyer *et al.* (1997) studied the α form at 208 K, using a single crystal grown *in situ* on a diffractometer by a zone-melting technique. Antson *et al.* (1987) determined the approximate structure of the deuterated β acetonitrile using a $C3v$ molecular model and neutron diffraction techniques. Crystal systems, space groups and cell dimensions for both α and β phases as determined by these authors are given in Table 1.

According to these authors, it proved impossible to grow single crystals of the β form below the transition temperature. Landau & Wurflinger (1980) attributed this fact to volume discontinuities at the transition. Following the preceding reports, more experiments were needed in order to reveal the structural changes accompanying the $\beta \rightarrow \alpha$ acetonitrile phase transition. In spite of its importance, the mechanism of such a transformation in molecular crystals remains open to discussion.

Here we report the single-crystal growth of β-CH_3CN and its X-ray crystal structure determination; an X-ray diffraction photograph of the ongoing $\beta \rightarrow \alpha$ transition; the structure refinement of the resulting α-CH_3CN single crystal; a description of a plausible mechanism for this transition.

In order to allow easier comparison between the structures, the temperatures of structural investigations have been set as close as possible to the phase-transition temperature, *i.e.* 206 K for the β form and 201 K for the α form.

Table 1
α and β acetonitrile crystallographic data from the literature.

	α-CH_3CN	α-CH_3CN	β-CH_3CN
Method	Single crystal	Single crystal	Powder
Reference	Barrow (1981)	Brackmeyer *et al.* (1997)	Antson *et al.* (1987)
Temperature (K)	215	208	100
Cell setting	Monoclinic	Monoclinic	Orthorhombic
Space group	$P2_1/c$	$P2_1/c$	$Cmc2_1$
a (Å)	4.11 (1)	4.103 (1)	6.05 (4)
b (Å)	8.27 (1)	8.267 (2)	5.24 (4)
c (Å)	7.98 (1)	7.969 (2)	7.79 (6)
β (°)	100.4 (2)	100.22 (2)	
V (Å^3)	266.8 (1)	266.0 (1)	246.9 (1)
Z	4	4	4

2. Experimental

A few drops of CH_3CN of reagent-grade quality (Carlo Erba 99.9%) were inserted into a Lindeman capillary; this operation was performed in a dry nitrogen atmosphere. The capillary was sealed in order to make a tiny cylindrical bubble of approximately 0.3 mm in diameter and 4 mm in length; the liquid took up 1.2 mm in length. The 'CH_3CN bubble', glued onto a fibreglass plate, was adjusted on a goniometric head and transferred onto a CAD-4 Nonius diffractometer. A steady nitrogen cold stream was blown onto the bubble using an in-house device allowing long-run experiments with a temperature control of ±0.1 K at any temperature in the range 100–300 K.

The preliminary crystal growth was conducted *in situ* by freezing CH_3CN at 187 K; then, using as a heater a tungsten electric wire mounted on a controlled displacement device, a single crystal was obtained using a gentle zone-melting technique, as described by Galy *et al.* (2002).

3. X-ray structure analysis

3.1. β-CH_3CN low-temperature form

The crystallization being achieved, the temperature was fixed at 206 K and the quality of the crystal was checked by a polaroid film technique. All the crystal and experimental data are summarized in Table 2. The extinction conditions clearly favoured the orthorhombic base-centred space groups *Cmcm*, *C2cm* or $Cmc2_1$. Analysis revealed that this crystal was the β form, a form claimed to be impossible to grow as a single crystal. The structure of β-CH_3CN was solved in the space group $Cmc2_1$ using Patterson and Fourier techniques, the C and N atoms being located first. The remaining H atoms were obtained *via* difference Fourier maps. C and N atoms were refined with their anisotropic displacement factors, but the H atoms were refined with only isotropic factors. The result is in general agreement with the structure previously deducted from powder neutron data. It is noted that, since the single-crystal data are collected at 206 K instead of 100 K for the Antson *et al.* (1987) powder analysis, the cell volume is larger by 4.4%. Bond lengths and angles are listed in the supplementary material.[1] All of the drawings containing molecules have been realized using the Burnett & Johnson (1996) software.

Table 2
Experimental details.

	β-CH_3CN	α-CH_3CN
Crystal data		
Chemical formula	C_2H_3N	C_2H_3N
Chemical formula weight	41.05	41.05
Cell setting, space group	Orthorhombic, $Cmc2_1$	Monoclinic, $P2_1/c$
a, b, c (Å)	6.187 (1), 5.282 (3), 7.887 (4)	4.102 (3), 8.244 (7), 7.970 (7)
β (°)	90	100.1 (1)
V (Å^3)	257.7 (2)	265.3 (4)
Z	4	4
D_x (Mg m^{-3})	1.058	1.028
Radiation type	Mo $K\alpha$	Mo $K\alpha$
No. of reflections for cell parameters	25	25
θ range (°)	5.68–20.11	5.20–21.48
μ (mm^{-1})	0.069	0.067
Temperature (K)	206 (2)	201 (2)
Crystal form, colour	Cylinder, colourless	Cylinder, colourless
Crystal size (mm)	1.2 × 0.5 × 0.3	1.2 × 0.5 × 0.3
Crystal radius (mm)	0.15	0.15
Data collection		
Diffractometer	Nonius CAD-4 diffractometer	Nonius CAD-4 diffractometer
Data collection method	ω–2θ scans	ω–2θ scans
No. of measured, independent and observed reflections	136, 136, 99	376, 324, 202
Criterion for observed reflections	$I > 2\sigma(I)$	$I > 2\sigma(I)$
$R_{\rm int}$	0.0000	0.0571
$\theta_{\rm max}$ (°)	24.91	21.89
Range of h, k, l	$0 \rightarrow h \rightarrow 7$ $0 \rightarrow k \rightarrow 6$ $-9 \rightarrow l \rightarrow 0$	$0 \rightarrow h \rightarrow 4$ $0 \rightarrow k \rightarrow 8$ $-8 \rightarrow l \rightarrow 8$
Refinement		
Refinement on	F^2	F^2
$R[F^2>2\sigma(F^2)]$, $wR(F^2)$, S	0.058, 0.1492, 1.155	0.0472, 0.1106, 1.107
No. of reflections and parameters used in refinement	136, 26	324, 41
H-atom treatment	All H-atom parameters refined	All H-atom parameters refined
Weighting scheme	$w = 1/[\sigma^2(F_o^2) + (0.0888P)^2 + 0.1685P]$ where $P = (F_o^2 + 2F_c^2)/3$	$w = 1/[\sigma^2(F_o^2) + (0.036P)^2 + 0.1879P]$ where $P = (F_o^2 + 2F_c^2)/3$
$(\Delta/\sigma)_{\rm max}$	0.037	0.000
$\Delta\rho_{\rm max}$, $\Delta\rho_{\rm min}$ (e Å^{-3})	0.176, −0.172	0.169, −0.168
Extinction method	*SHELXL*	*SHELXL*
Extinction coefficient	0.01 (7)	0.07 (4)

Computer programs used: *CAD*-4-*EXPRESS* (Enraf–Nonius, 1993), *CADAK* (Savariault, 1991), *SHELXS*96 (Sheldrick, 1990), *SHELXL*96 (Sheldrick, 1996).

---

[1] Supplementary data for this paper are available from the IUCr electronic archives (Reference: OS0098). Services for accessing these data are described at the back of the journal.

3.2. β-CH_3CN crystal structure

The N atom, the C2 and C1 atoms, and the H1 atom lie on the mirror plane m perpendicular to the [100] direction, while H2 and the related H2^{i} lie out of the plane (Fig. 1). As $Cmc2_1$ is a polar space group, the origin along [001] has been fixed on C2, *i.e.* $z = 0$*. The molecular axes are arranged along the [010] direction (see Fig. 2) and are packed in layers parallel to (100) with $a/2$ periodicity, as shown in Fig. 3.

The molecules are parallel in the same layer and are packed head-to-tail with the sandwiching layers. As expected, C2 vibrates along the $N-C2-C1H_3$ molecular axis and the C—C and C≡N distances are typical of single and triple bonds. The easy localization by Fourier difference of the H atoms indicates that there is no disorder of the CH_3 groups.

The lone pair E of the N atom, lying with the molecule in the mirror plane, is directed towards the tail of the molecule related by the helicoidal axis (coordinate transformation $0, y, z \rightarrow 0, -y, z - \frac{1}{2}$) and more particularly towards C1 on the bisecting angle H2—C1—H2^{i}. The axes of both molecules are roughly perpendicular (Fig. 2). N$^{ii}\cdots$H2^{iii} and N$^{ii}\cdots$H2^{iv} interactions [2.69 (7) Å] with molecules located in the mirror plane at $a = \pm 0.5$ strengthen the structure in the [100] and [001] directions. N$^{ii}\cdots$H1^{v} [2.79 (8) Å] interactions between N and H atoms of neighbouring molecules at the same level along the [010] direction complete this three-dimensional arrangement formed by the molecular packing.

In the mirror planes m, alternately ($b/2$ period), the $-CH_3$ groups and the N atoms and their lone pairs E (NE entities) pack along the helicoidal twofold axis. The N$\cdots$H interactions between consecutive mirror planes show how the cohesion of the structure is ensured along the [100] direction.

3.3. The $\beta \rightarrow \alpha$ phase transition

With the crystal data of β-CH_3CN being recorded and the quality preliminarily checked *via* polaroid film (Fig. 4*a*), the temperature of the single crystal was gently raised to 211 K over 30 min. Meanwhile, an X-ray image was collected on the polaroid film over 15 min, with the crystal rotating around the φ axis aligned with both ω and θ axes ($\kappa = 0°$). Comparing Fig. 4(*b*) with the image collected (with the same diffractometer adjustment) for the β form (Fig. 4*a*) shows that the crystal was undergoing a phase transition. Fig. 4(*c*) indicates that this transition period was achieved and concluded by a complete transformation of the β-CH_3CN form into a new crystal, which was established to correspond to the α-CH_3CN form.

3.4. α-CH_3CN high-temperature form

Continuing our X-ray investigations on the same crystal after its transformation, it was demonstrated that it was the α

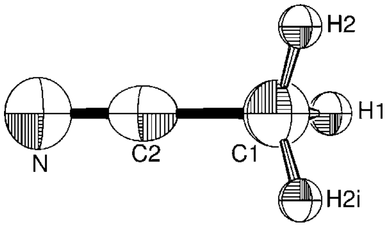

Figure 1
The β-CH_3CN molecule with a mirror plane symmetry. Symmetry code: (i) $-x, y, z$. Ellipsoids are drawn at the 85% probability level.

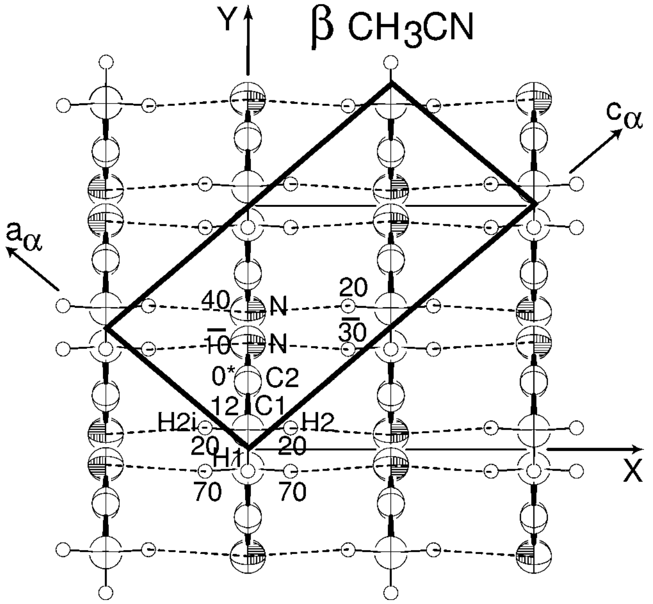

Figure 2
Projection onto the (001) plane of the β-CH_3CN structure.

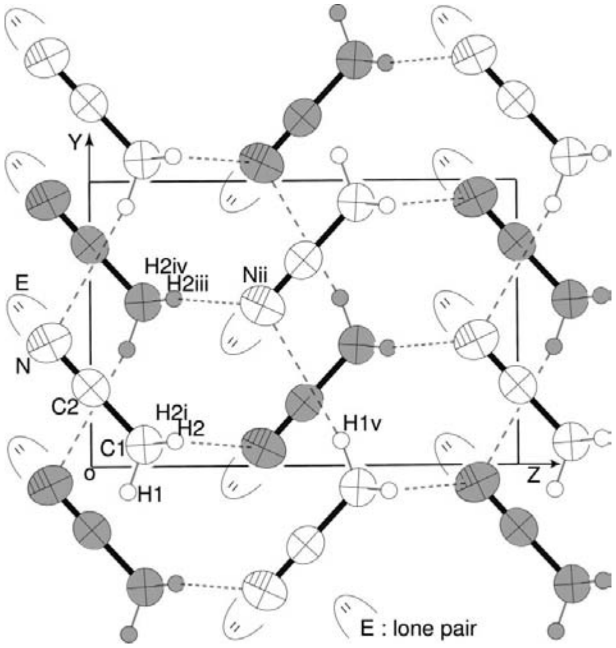

Figure 3
Projection onto the (100) plane of the β-CH_3CN structure. Symmetry codes: (i) $-x, y, z$; (ii) $x, -y + 1, z + \frac{1}{2}$; (iii) $-x + \frac{1}{2}, y + \frac{1}{2}, z$; (iv) $x - \frac{1}{2}, y + \frac{1}{2}, z$; (v) $x, -y, z + \frac{1}{2}$.

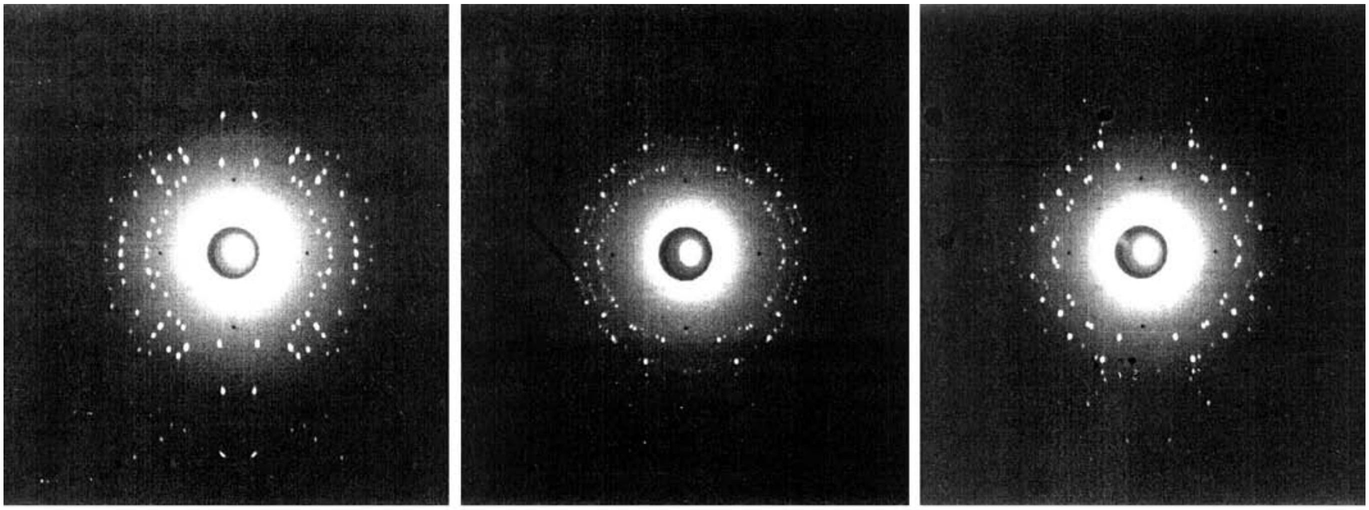

(*a*) (*b*) (*c*)

Figure 4
X-ray polaroid photographs of the CH_3CN crystal: (*a*) β form; (*b*) transition period; (*c*) α form.

form of CH_3CN, structurally depicted by Barrow (1981). This latter work was performed using a Weissenberg camera and Cu $K\alpha$ radiation, the crystal being cooled and maintained at 215 K. Brackmeyer *et al.* (1997) confirmed this work in their single-crystal study at 208 K on an automatic diffractometer.

On obtaining such a good crystal after the transition, it was decided to take the opportunity to refine its structure, in order to facilitate comparisons with the β form and to understand the ongoing molecular mechanism. Taking advantage of the hysteresis in the $\beta \rightarrow \alpha$ transformation, which was already observed by Putnam *et al.* (1965), the temperature of the crystal was slightly diminished and maintained at 201 K during data collection. After this study, the crystal was cooled to a lower temperature but it kept its polymorphic α form.

The α-form data collection and structural determination and refinements were performed in the same way as those used for the β form (see Table 2).

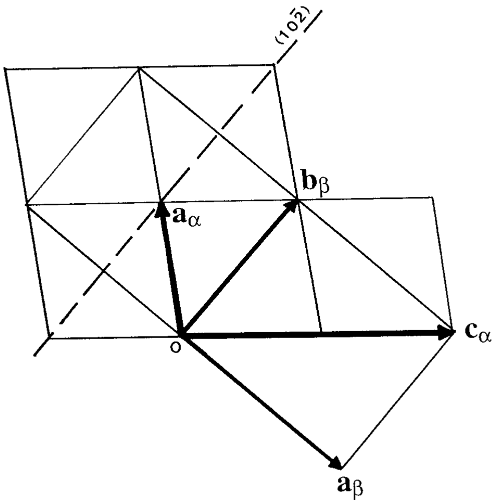

Figure 5
Geometric cell relations between the α and β forms.

4. Discussion

The relationships between the cell parameters of the two forms are as follows:

$$\mathbf{a}_\alpha = (-\mathbf{a}_\beta + \mathbf{b}_\beta)/2,$$

$$\mathbf{b}_\alpha = 1.045\mathbf{c}_\beta,$$

$$\mathbf{c}_\alpha = \mathbf{a}_\beta + \mathbf{b}_\beta.$$

These relationships are illustrated in Fig. 5. The calculated parameters of the α form based on those of the β form (Table 2) are $a_\alpha \simeq 4.07$, $b_\alpha \simeq 8.24$, $c_\alpha \simeq 8.14$ Å and $\beta_\alpha \simeq 99^\circ$, in good agreement with those found for the crystal. The cell volumes V_α and V_β are rather close, V_α being approximately 3% larger, which is reasonable for the high-temperature form.

The structure determination of the α form is in good agreement with the structures determined by Barrow (1981) and Brackmeyer *et al.* (1997). Fig. 6, a projection onto the (010) plane, shows that the molecules lie in layers along the $(10\bar{2})$ planes. The molecules have lost their crystallographic mirror planes but maintain their repetition along $(10\bar{2})$ *via* the helicoidal twofold axis 2_1 for the tail $-CH_3$ groups and the symmetry centre between the heads, *i.e.* N*E*. The CH_3CN molecules are now head-to-head, with pairs of molecules associated *via* the symmetry centre and, after a slight tilting, repeated *via* the 2_1 axis. The H1 atom is always situated in the pseudo mirror plane of the molecule while the other two H atoms are now crystallographically independent, *i.e.* H2 and H3.

The lone pair *E* of the N atom points in the direction of the $H1^{ii}$ atom of a molecule translated by the vector $\mathbf{v} = \mathbf{a} + \mathbf{c}/2$. The values of the angle $C2-N-H1^{i}$ [171.7 (11)°] and the interatomic distance $N\cdots H1^{ii}$ [2.60 (4) Å] indicate an interaction, the sum of the van der Waals radii (VWR) being 2.75 Å (r_{VWR} of C = 1.70, N = 1.55 and H = 1.20 Å).

Table 3
Selected geometric parameters (Å, °) for the β form of acetonitrile.

N—C2	1.149 (12)	C1—H1	1.02 (8)
C1—C2	1.436 (12)	C1—H2	1.11 (7)
C2—C1—H1	117 (6)	H1—C1—H2	103 (4)
C2—C1—H2	110 (3)	N—C2—C1	178.9 (12)

It is noted that the number of N···H interactions between the molecules of one layer and those of the contiguous layers is halved. A comparison is made (dotted lines) in Fig. 6. This indicates an increased fragility of the network, which results in a slightly higher melting point (227 K).

The intramolecular bonding does not show significant discrepancies, the bonds in both forms being almost identical (Tables 3 and 4). The C—H bonds are remarkably regular in the α form, $\pm$ 0.06 Å around an average C—H = 1.02 Å (Table 3). The H···H interatomic distance between CH_3 groups is 1.61 (5) Å.

The C1···N distance [2.59 Å] is the same in both forms. In the head-to-head $H_3C—C1—NE\cdots EN—C1—C2H_3$ positioning, the lone pairs are nicely packed along the corresponding c_β or b_α axes. This lone-pair packing and its stereochemical role, very often encountered in solid-state structures in which elements are characterized by an ns^2 electronic state, has been emphasized by Galy *et al.* (1975) and Galy & Enjalbert (1982).

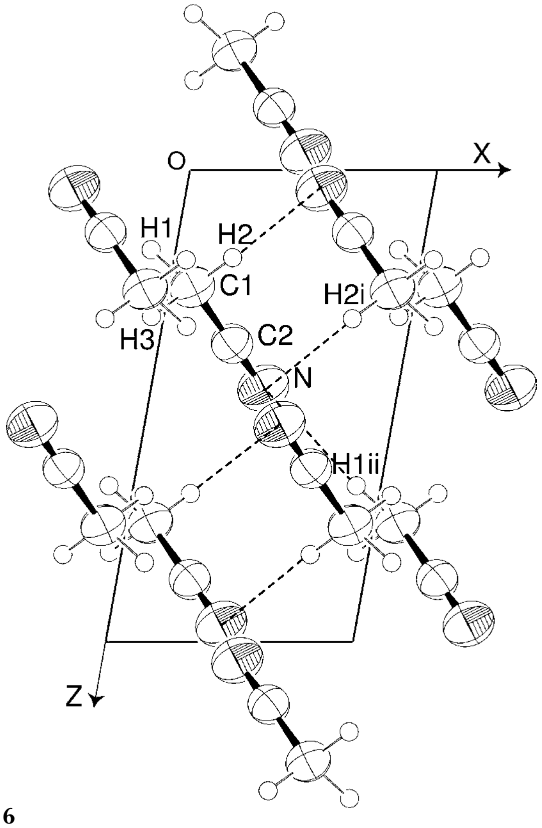

Figure 6
Projection onto the (010) plane of the α-CH_3CN structure. Symmetry codes: (i) $-x+1, y-\frac{1}{2}, -z+\frac{1}{2}$; (ii) $x+1, -y+\frac{1}{2}, z+\frac{1}{2}$.

Table 4
Selected geometric parameters (Å, °) for the α form of acetonitrile.

N—C2	1.141 (5)	C1—H2	0.96 (5)
C1—C2	1.448 (6)	C1—H3	1.03 (5)
C1—H1	1.07 (5)		
C2—C1—H1	115 (2)	H1—C1—H3	95 (3)
C2—C1—H2	110 (3)	H2—C1—H3	108 (4)
H1—C1—H2	112 (3)	N—C2—C1	179.3 (4)
C2—C1—H3	115 (2)		

Fig. 7 allows us to propose a mechanism for the $\beta \rightarrow \alpha$ structural transformation. Let us select the molecules lying in a mirror plane in the β form. A double string of the molecular sequence developed along [001] and repeated with a periodicity, b, of 5.282 (3) Å along [010] is indicated by a grey background. The same type of sequence is illustrated for the α form using the molecules lying in the $(10\bar{2})$ plane, again taken with a 2 $\times$ 5.194 (4) Å periodicity. Let us fix these molecules. Between these double strings we are left with a double

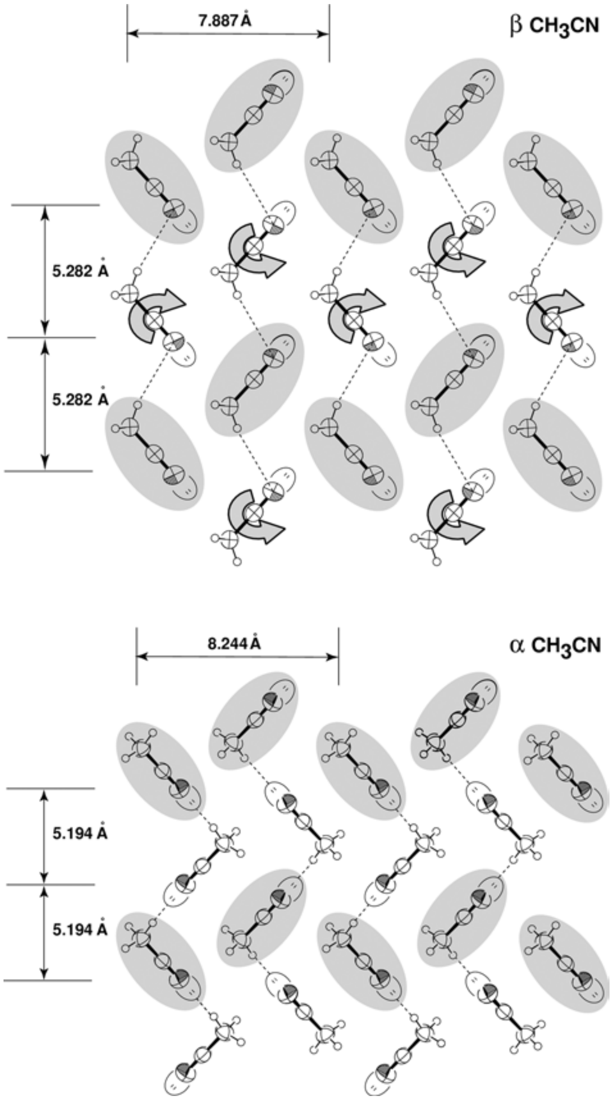

Figure 7
Mechanism proposed for the $\alpha \rightarrow \beta$ phase transition.

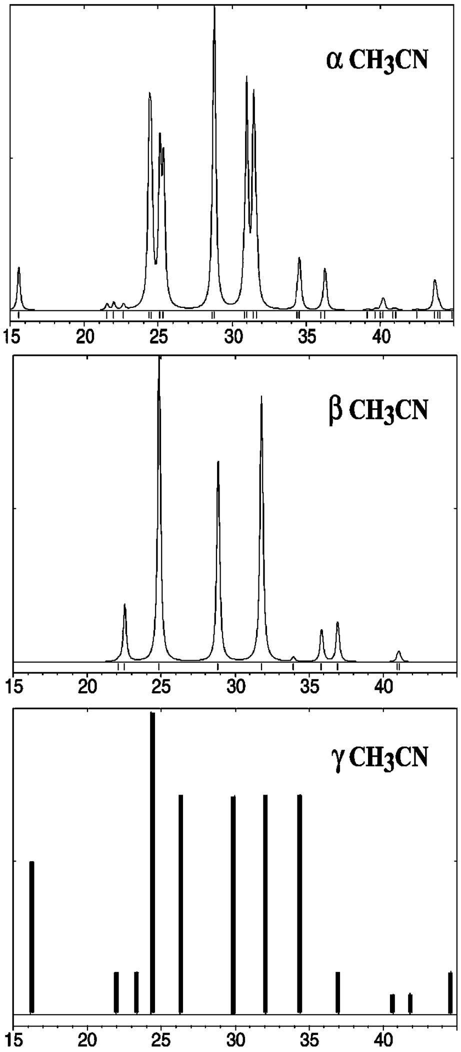

Figure 8
Calculated powder patterns for *α* and *β* forms together with that constructed based on Pace & Noe (1968) data for acetonitrile directly quenched in liquid nitrogen.

sequence of CH_3CN molecules packed head-to-tail. Now, if in the *β* form a cooperative rotation of about 90° is applied to the molecules (according to the arrows) then the general organization of the *α* form is obtained. Such movement gives roughly the same periodicity along the [001] direction, *i.e.* 5.194 (4) Å against 5.282 (3) Å and an expansion along the $[20\bar{1}]$ direction from 7.887 (4) Å to 8.244 (7) Å.

5. Conclusion

For the first time, the *β* form of CH_3CN has been obtained and its structure determined *via* X-ray single-crystal analysis. The results confirm the general description issued from powder neutron diffraction techniques. A simple mechanism has been proposed to transform this *β* form into the *α* form, based on a 90° rotation of every double slab of molecules packed in layers.

To conclude, we calculated the X-ray powder patterns of both phases using the *PowderCell* software (Kraus & Nolze, 1999). These are reported in Fig. 8. We also simulated the powder pattern reported by Pace & Noe (1968) for acetonitrile enclosed in a Lindeman capillary directly dipped in liquid nitrogen (*vw*, *w*, *m*, *s* and *vs* intensities were roughly schematized). It appears that the powder pattern is not fitted by either *α* or *β* data. Does a third polymorph of CH_3CN exist?

References

Antson, O. K., Till, K. J. & Andersen, N. H. (1987). *Acta Cryst.* B**43**, 296–301.

Barrow, M. J. (1981). *Acta Cryst.* B**37**, 2239–2242.

Brackmeyer, T., Erker, G., Fröhlich, R., Prigge, J. & Peuchert, U. (1997). *Chem. Ber. Rec.* **130**, 899–902.

Burnett, M. N. & Johnson, C. K. (1996). *ORTEPIII.* Report ORNL-6895. Oak Ridge National Laboratory, Tennessee, USA.

Enraf-Nonius (1993). *CAD*-4-*EXPRESS.* Version 5.1. Enraf-Nonius, Delft, The Netherlands.

Galy, J. & Enjalbert, R. (1982). *J. Solid State Chem.* **44**, 1–23.

Galy, J., Enjalbert, R., Lecante, P. & Burian, A. (2002). *Inorg. Chem.* **41**, 693–698.

Galy, J., Meunier, G., Andersson, S. & Aström, S. (1975). *J. Solid State Chem.* **13**, 142–159.

Kraus, W. & Nolze, G. (1999). *Powder Cell Software.* Version 2.4. Federal Institute for Material Research and Testing, Berlin, Germany.

Landau, R. & Wurflinger, A. (1980). *Ber. Bunsenges. Phys. Chem.* **84**, 895–902.

Pace, E. L. & Noe, L. J. (1968). *J. Chem. Phys.* **49**, 5317–5325.

Putnam,W. E., McEachern, D. M. & Kilpatrick, J. E. (1965). *J. Chem. Phys.* **42**, 749–755.

Savariault, J. M. (1991). *CADAK. Data Reduction.* CEMES, Toulouse, France.

Sheldrick, G. M. (1990). *Acta Cryst.* A**46**, 467–473.

Sheldrick, G. M. (1996). *SHELXL*96. *Program for the Refinement of Crystal Structures.* University of Göttingen, Germany.